

Parameters Design and Finite Element Analysis of Single Phase Excitation 8/6 Poles Switched Reluctance Motor

Chuanyu Sun ^{1, a}, Jingkai Li ^{1, b}, Te Xu ^{1, c} and Maoyong Cao ^{2, a}

¹Shandong University of Science and Technology, Qingdao 266590, China;

²Graduate School, Shandong University of Science and Technology, Qingdao 266590, China.

^asuncy2011@yeah.net, ^b13563222177@163.com

Abstract

In this paper, the structure and operation principle of the single-phase excitation 8/6 poles switched reluctance motor (SRM) were described, and the mathematical model were deduced. According to the parameters design principle of the SRM, established a prototype motor in Ansys maxwell, which rated power is 5 kw. Through the electromagnetic simulation, curve cluster of the flux linkage and curves of torque were obtained, compared the simulation results with the mathematical model, and finally proved the correctness of parameters design.

Keywords

Switch reluctance motor; Mathematical model; Parameters design; Finite element analysis.

1. Introduction

Switched reluctance motor (SRM) is an advanced electromechanical integration device, which has advantages such as simple structure, low cost, body strong, high reliability and wide speed range[1, 2]. Nowadays, the SRM has been widely used in electric vehicle[3], mine, oilfield, textile machinery and other industrial areas, and it is of great significance to improve the performance of the production equipment. However, the unreasonable design of the motor structure parameter often leads to problems such as low energy utilization rate, serious body loss and with large ripple of the output torque[4]. This paper focus on the single phase excitation 8/6 pole SRM, in section 2, described the structure and operation principle, in section 3, deduced the mathematical model and given the specific parameters, in section 4, the experimental prototype was established in Ansys Maxwell 2D, compared the simulation results with mathematical model and finally proved the correctness of parameters design, and the conclusion were given in section 5.

2. Structure and Operation Principle

In this paper, the SRM adopts the structure of double salient pole tooth both of stator and rotor, and the number of stator teeth and rotor teeth are different. 8/6 poles structure is commonly used in SRM, the stator has 8 teeth ($N_s = 8$) and stator teeth distributed in circular array, each tooth has a coil wound around it, the coils which opposed diametrically form a phase winding in series, and there are four phase windings A, B, C, and D. The rotor has 6 teeth ($N_r = 6$) and rotor teeth distributed in circular array, there are no coils wound around the rotor teeth. Since the inductance is inversely proportional to the magnetic resistance, when the center line of rotor teeth is aligned with the center line of stator teeth, the inductance of phase winding is the largest, and when the center line between rotor teeth is aligned with the center line of stator teeth, the inductance of phase winding is the smallest.

The operation principle of single-phase excitation of 8/6 poles SRM is shown in Fig. 1, where S1 and S2 are electronic switches, VD1 and VD2 are freewheeling diode, and E is dc power. In the first stage,

at the position shown in Fig. 1, S1 and S2 are closed, and the A phase winding are energized, assume that the overlap angle of the rotor is θ (define the position which center line of the rotor teeth is aligned with the center line of the stator teeth is $\theta=0^\circ$, and clockwise direction is positive). The rotor rotates clockwise along the axis due to the tangential electromagnetic force, until the center line of rotor teeth is aligned with the center line of stator teeth, during this process, the rotor rotated 15 degrees[5, 6]. In the second stage, the S1 and S2 of B are closed while S1 and S2 of A phase are shut off, and the B phase winding are energized. The windings are energized periodically in the order of A-B-C-D-A and the rotor will rotate clockwise continuously. Each phase winding will be energized at θ and shut off when $\theta_1=\theta+15^\circ$, therefore, the rotor rotates 60o per electrical cycle.

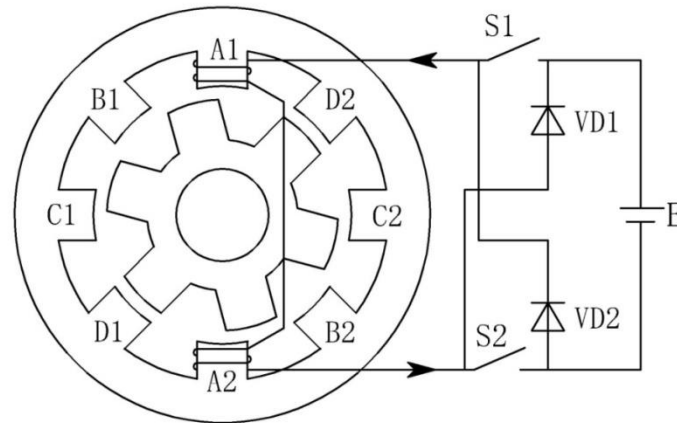


Fig 1. Operation principle of single phase excitation 8/6 poles SRM

3. Mathematical Model and Parameters Design

3.1 Mathematical Model

Since the structure and parameters of all phase windings are theoretically the same for a SRM, the voltage balance equation of k phase winding can be expressed as:

$$U_k=R_k \cdot i_k + \frac{d\Psi_k}{dt} \tag{1}$$

where U_k , R_k , i_k , and Ψ_k respectively represent the phase winding terminal voltage, resistance, current and flux linkage of the k phase.

The flux linkage Ψ_k is determined by some factors such as the k phase current i_k , self-inductance L_k , the others phase current i_o , mutual inductance and rotor position angle θ , L_k is determined of i_k and θ . Since the mutual inductance between windings is far less than the self-inductance, the calculation process is generally simplified by ignoring the mutual inductance. Therefore, the flux linkage equation can be expressed as:

$$\Psi_k=L_k(i_k, \theta)i_k \tag{2}$$

In the ideal state, the nonlinearity of the magnetic circuit is not considered, equation (2) can be substituted into (1) to obtain:

$$U_k=R_k \cdot i_k + \left(L_k + i_k \frac{\partial L_k}{\partial i_k} \right) \frac{di_k}{dt} + i_k \frac{\partial L_k}{\partial \theta} \omega \tag{3}$$

It can be seen from equation (3) that the power voltage is equal to the voltage drop of the other three parts of the circuit. The first term on the right side of the equation is the voltage drop of the resistance of k phase loop. The second term is the induced electromotive force, which caused by the change of the flux linkage, and the change of the flux linkage is caused by the change of current. The third term is also the induced electromotive force, which related to the energy conversion of SRM and caused by the change of the flux linkage, but the change of the flux linkage is caused by the change of the rotor position.

According to the electromechanical energy conversion principle, the electromagnetic torque of SRM can be expressed as the partial derivative of the magnetic co-energy to the rotor position angle θ :

$$T_k = \frac{\partial W_m(i_k, \theta)}{\partial \theta} = T(i_k, \theta) \quad (4)$$

Through mechanical analysis, it can be concluded that under the action of electromagnetic torque and load torque, the mechanical motion equation of the rotor can be expressed as:

$$J \frac{d\omega}{dt} = \sum_{k=1}^m T_k - T_l - F\omega \quad (5)$$

Where J is the moment of inertia, ω is the mechanical rotating angle, T_k is the the electromagnetic torque of k phase, T_l is the load torque of k phase, F is damping coefficient.

3.2 Parameters design

According to the parameters design principle of SRM, the basic relationship between parameters can be obtained:

Average current of per phase

$$I_{ka} = \frac{P}{m\eta U} I_{ka} = \frac{P}{m\eta U} \quad (6)$$

Air-gap permeance between the stator teeth and rotor teeth

$$I_{ka} = \frac{P}{m\eta U} \wedge = \frac{\mu S}{l} = \frac{\mu h r}{l} \left(\frac{\pi}{8} + \theta \right) \quad (7)$$

Self-induction

$$L = 4N^2 \wedge \quad (8)$$

Average output torque of SRM

$$T_{ka} = \frac{mN_r}{2\pi} \int_0^{2\pi} T_k(\theta, i(\theta)) d\theta \quad (9)$$

Rated torque of SRM

$$T_n = \frac{P}{n \frac{2\pi}{60}} = \frac{30P}{\pi n} = \frac{mT_{ka}}{2} \quad (10)$$

Where P is the rated power, m is the phase number, η is the efficiency, U is the input voltage, μ is the permeability of vacuum and $\mu = 4\pi \cdot 10^{-7} \text{H/m}$, S is the area of the facing parts of the stator teeth and rotor teeth, l is the thickness of air gap, N is the number of coil turns, h is the axial length of SRM, r is the outer diameter of the rotor, θ is the position angle of the rotor, n is the speed of rotor.

According to formula (1)-(10), the electrical parameters of the SRM can be obtained by analyzing the relationship between motor parameters. In this paper, the rated power P is 5 kw, the rated speed $n=5000\text{r/min}$. In addition, the other parameters such as the pole-arc coefficient of the stator teeth and rotor teeth, the inner and outer diameter of the stator and rotor, the thickness of air gap, etc., the derivation and calculation of these parameters are relatively simple and don't list the specific calculation process. The results of the mechanical parameters and electrical parameters are shown in Table 1.

4. Simulation and Analysis

According to the data listed in Table 1, the experimental prototype was established in Any's Maxwell 2D and performed finite element simulation. Fig 2 shows the curve cluster of the flux linkage obtained by finite element simulation, and it can be seen from Fig 2 that the characteristics of the flux linkage is determined by the rotor position θ , through the simulation of the experimental prototype, the paper reached the opposite flux linkage in different rotor positions and forms the curve cluster of the flux linkage. In Fig 2, the horizontal coordinate is current, the vertical coordinate is flux, and from the bottom to top respectively represent rotor position 0° , 2.5° , 5° , 7.5° , 10° , 12.5° and 15° . When θ is 0° , the center line of the rotor teeth are aligned with the center line between stator teeth, the inductance of phase winding and the air gap permeance are both the smallest, the iron core is unsaturated, and the flux linkage is proportional to the current. As the increase of θ , the saturation of the flux linkage and air gap permeance are both increase. When θ is 15° , the entire area of stator teeth are opposite to the rotor teeth, the inductance of phase winding and air gap permeance are both the largest, at this

position, the saturation rate of the iron core is the fastest, and with the increase of current, the flux linkage has presented distinct nonlinear characteristics.

Table 1. Basic parameters of the 8/6 poles SRM

Parameter Name	Number	Units	Symbol
Rated power	5	KW	P
Rated speed	5000	r/min	n
Phase number	4	/	q
Outer diameter of the stator	72	mm	r_{so}
Inner diameter of the stator	42.9	mm	r_{si}
Pole-arc coefficient of the stator	0.42	%	β_s
Height of stator teeth	17.1	mm	/
Outer diameter of the rotor	42.5	mm	r
Inner diameter of the rotor	16	mm	r_{ri}
Height of rotor teeth	12	mm	/
Pole-arc coefficient of the rotor	0.42	%	β_r
Axial length	102	mm	h
Thickness of air gap	0.4	mm	l
Current	4	A	i
Number of coil turns	300	/	N
Efficiency	88	%	η
Step angle	15	$^\circ$	/
Rated torque	9.5	N·m	T_n

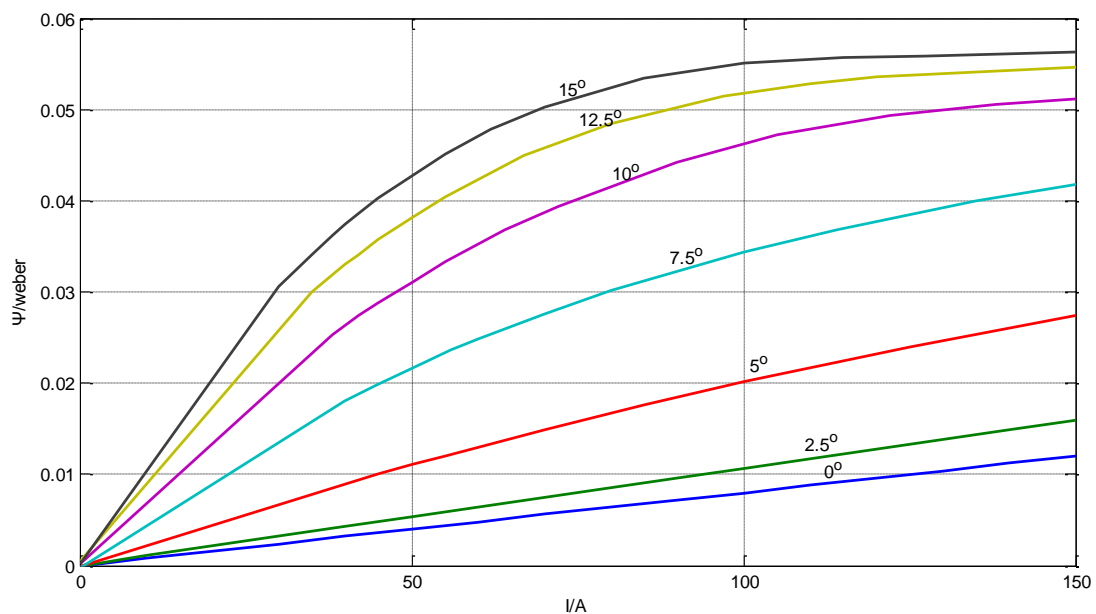


Fig 2. Curve cluster of the flux linkage

Fig 3 (a) shows the distribution of magnetic induction lines when θ is 7.5o, the direction and density of the magnetic induction line can be found from it. Fig 3 (b) is the flux density when θ is 7.5o, and it shows the strength of the magnetic field. From the comparison between Fig 3 (a) and Fig 3 (b), it can be seen that the variation trend of magnetic field is exactly the same as the distribution of magnetic induction lines. It can be found in Fig 3 that there is a certain magnetic saturation in the opposite facing area of the stator teeth rotor teeth and the other areas are unsaturated.

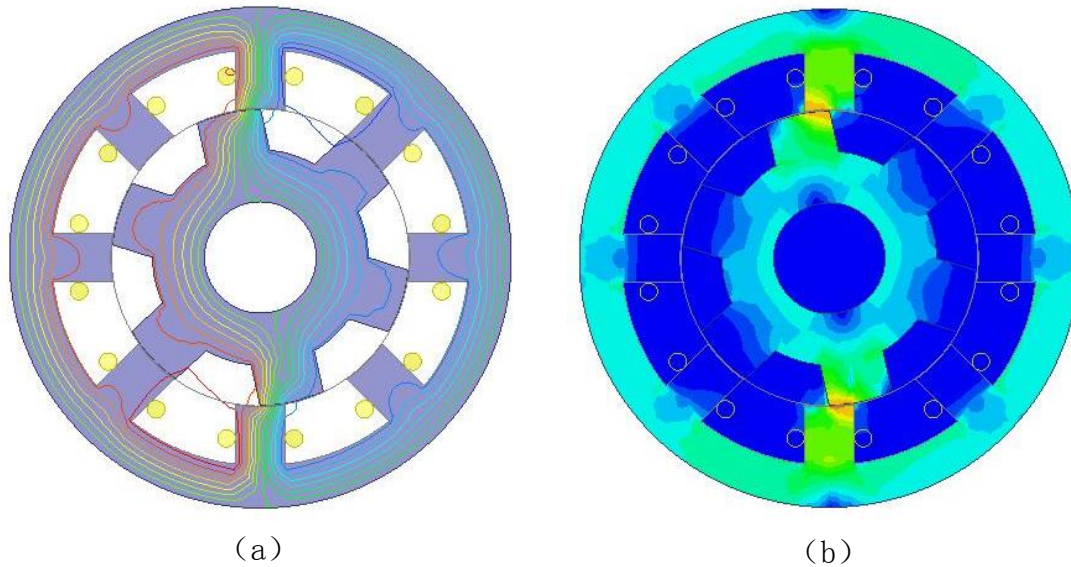


Fig 3. Distribution of magnetic induction lines and flux density

Fig 4 shows the output torque of the mathematical model and simulation. It can be found from Fig 4 that the simulation result has a large ripple when θ from -15° to -12° , which is not consistent with the mathematical model, but from -12° to 0° , the mathematical model and simulation result have a good fitting degree, this phenomenon is caused by the current break during the start-up and commutation. In the whole range, the fitting degree nearly reaches 80%, hence, it can be considered that the simulation result approximately equals the mathematical model.

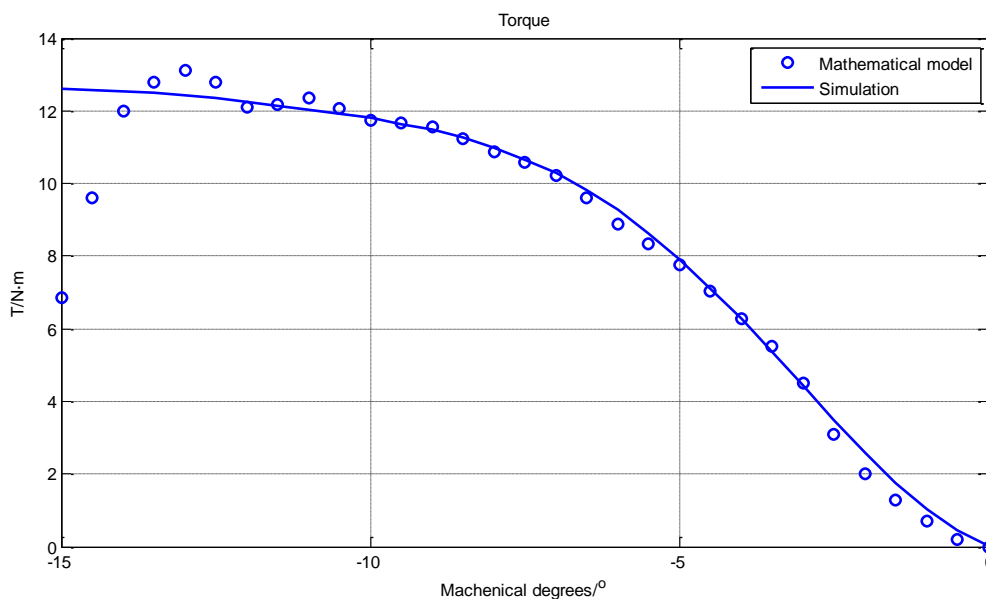


Fig 4. Output torque of the mathematical model and simulation

In order to reduce the torque ripple during commutation, the range of energization is set as $(-17^\circ, -2^\circ)$. Fig 5 shows the waveform curve of output torque in one electrical cycle, it can be seen from the waveform that the peak output torque of the proposed SRM is $13\text{N}\cdot\text{m}$, slightly larger than the calculated value. The average torque output is about $9.2\text{N}\cdot\text{m}$, and consistent with the calculation value. However, the output torque ripple of the proposed SRM is too large and still needs to be optimized.

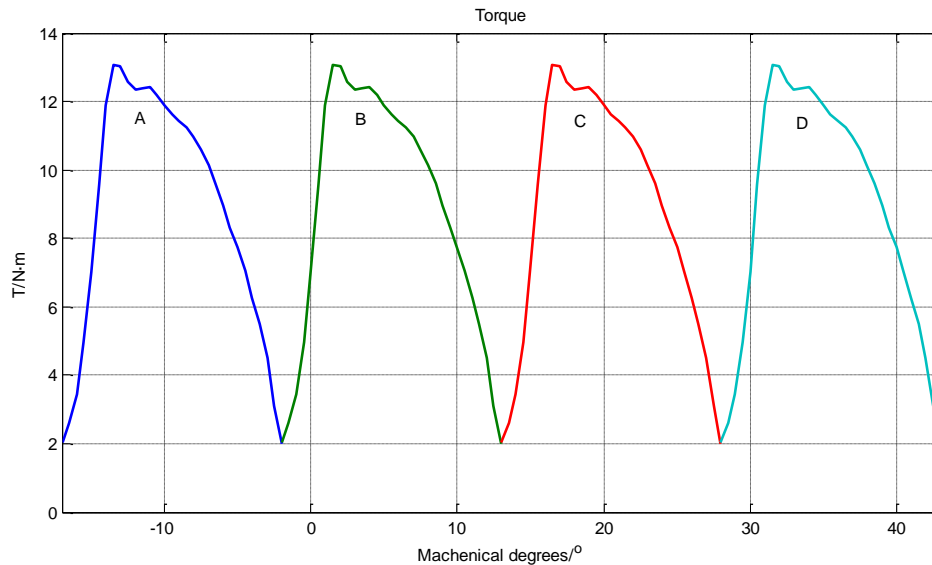


Fig 5. Waveform of the output torque

According to the analysis of Fig 3, Fig 4 and Fig 5, it can be concluded that based on the parameters listed in Table 1, the correct magnetic circuit and output torque can be obtained through the finite element simulation, meanwhile, the correctness of the parameters design of the single phase excitation 8/6 poles SRM can be verified.

5. Conclusion

The paper introduced the structure and operation principle of SRM, derived its universal mathematical model and provided the parameters design method. According to the parameters design method, a single phase excitation 8/6 poles SRM is designed, which rated power is 5kW, the specific parameters are calculated. Finally, the electromagnetic characteristics of the SRM were obtained by finite element simulation, and the simulation results verified the correctness of parameters design.

Acknowledgements

In this paper, the research was sponsored by Qingdao Application Research Project of Shandong Province (Project No. 15-9-1-66-jch), Qingdao Postdoctoral Research Foundation of Shandong Province (Project No. 01020120521), and Coal Industry Association Scientific Research Project of China (Project No. MTKJ 2015-237).

References

- [1] Y.K. Sun, Y. Yuan, Y.H. Huang, et al. Development of the bearing less switched reluctance motor and its key technologies, Transactions of China Electro technical Society, vol. 30 (2015), 1-8.
- [2] W. Peng, F.G. Zhang, et al. Design and control of a novel bearing less SRM with double stator, IEEE International Symposium on Industrial Electronics, 2012, 1928-1933.
- [3] L.J. Xiao, B. Li, C.Y. Sun, et al. Torque mathematic model of 8/6 switched reluctance motor with single phase excitation, Industry and Mine Automation, vol. 42 (2016), 62-66.
- [4] L. Bo, L.J. Xiao, C.Y. Sun, et al. Torque mathematic model of 8/6 switched reluctance motor with two winding excitation, Small & Special Electrical Machines, vol. 44 (2016), 19-25.
- [5] Y.J. Zhao, B. Li, X.B, et al. Design and simulation of extra-high voltage switched reluctance motor with three phase 12/8 poles, vol. 31 (2014), 20-23.
- [6] Y. Zhang, Z.Q. Deng. Design and realization of bearing less switched reluctance motor, Act Aeronautic ET Astronautic Sonica, vol. 27 (2006), 77-80.